J|A|C|S
ARTICLES
Published on Web 04/21/2006

High Resolution Spectral Differentiation of Enantiomers: Benzo[*a*]Pyrene Tetrols Complexed with a Promiscuous Antibody

Nenad M. Grubor,[†] Ying Liu,[†] Xinxin Han,[‡] Daniel W. Armstrong,[‡] and Ryszard Jankowiak*,[§]

Contribution from the Department of Chemistry, Iowa State University, Ames, Iowa 50011, Department of Chemistry and Biochemistry, University of Texas at Arlington, Arlington, Texas 76019, and Department of Chemistry, Kansas State University, Manhattan, Kansas 66502

Received December 12, 2005; E-mail: ryszard@ksu.edu

Abstract: The interaction of the highly cross-reactive *anti*-PAH monoclonal antibody with four diastereomeric benzo[*a*]pyrene tetrols (BPTs) is studied by means of fluorescence line-narrowing spectroscopy. It is shown that the interaction of enantiomers of *cis*-BPT and *trans*-BPT with the antibody involves different complex geometries. These spatially different ligand−protein interactions alter the relative intensities of the excited-state vibrational frequencies of immunocomplexed molecules allowing for unambiguous spectroscopic resolution of all four enantiomeric isomers. This study represents the first example of a high-resolution, fluorescence-based spectroscopic method capable of enantiospecific differentiation.

Introduction

Although antibody−antigen interaction is known to be one of the most specific recognition events in nature, examples of nonspecific (cross-reactive) antibodies are numerous.[1−3] While antibody cross-reactivity has been assigned an important physiological role (i.e., in immunological versatility, autoimmunity, allergy), it is also critical for immunoanalytical methods that rely exclusively on antibodies' discriminative properties. Constrained by the impotence of conventional immunochemical detection techniques to differentiate between "desired" and "false" binding events, cross-reactivity may be detrimental to the validity of an immunoassay. The question arises as to whether the combination of the cross-reactive immunocomplexation and a highly selective, information-rich detection method could provide the required selectivity even with nonspecific immunoassays. While information-rich detection methods (such as mass spectrometry, NMR spectroscopy, wavelength-resolved UV−vis spectroscopy, high-resolution fluorescence and Raman spectroscopies) have found their place in integrated analytical schemes (through hyphenation with various modes of chromatography and electrophoresis[4]), immunoanalytical formats remain reliant on one-dimensional, noninformative signals. We have recently demonstrated that high-resolution spectroscopy, i.e., fluorescence line-narrowing spectroscopy (FLNS), coupled with analytical separation techniques[4] and biosensors[5] successfully differentiates between structurally similar analytes, thus precluding potential qualitative analytical ambiguities.

From the perspective of the specificity of an analytical method, chiral differentiation is probably the most challenging issue and requires involvement of another chiral element: a chiral molecule or circularly polarized electromagnetic wave. Molecular chirality and enantioselectivity are fundamental aspects of biological activity and are reflected in remarkable discriminatory, antagonistic, or side physiological effects of enantiomeric analogues.[6−8] Chemically induced carcinogenesis, for example, has been shown to evolve from enantioselective DNA damage initiated by prochiral mutagenic agents.[9] The development of techniques that are capable of diastereomeric differentiation is crucial not only from a bioanalytical (diagnostic) standpoint, but also from the perspective of understanding the mechanism(s) that underlie enantioselective biological interactions. However, both conventional low- and high-resolution spectroscopic techniques (based on randomly polarized excitation sources) are incapable of distinguishing between enantiomeric analogues.

Here we show that the integration of high-resolution fluorescence spectroscopy (i.e., FLNS) in an immunoassay allows for differentiation of cross-reactively immunocomplexed species.

[†] Iowa State University.
[‡] University of Texas at Arlington.
[§] Kansas State University.

(1) James, L. C.; Roversi, P.; Tawfik, D. S. *Science* **2003**, *299*, 1362−7.
(2) Arevalo, J. H.; Taussig, M. J.; Wilson, I. A. *Nature (London)* **1993**, *365*, 859−62.
(3) Ekins, R. *Nature* **1989**, *340*, 256−258.
(4) Jankowiak, R.; Roberts, K. P.; Small, G. J. *Electrophoresis* **2000**, *21*, 1251−66.
(5) Grubor, N. M.; Shinar, R.; Jankowiak, R.; Porter, M. D.; Small, G. J. *Biosens. Bioelectron.* **2004**, *19*, 547−556.
(6) Armstrong, D. W.; Ward, T. J.; Armstrong, R. D.; Beesley, T. E. *Science* **1986**, *232*, 1132−5.
(7) Eichelbaum, M.; Gross, A. S. *Adv. Drug Res.* **1996**, *28*, 1−64.
(8) Islam, M. R.; Mahdi, J. G.; Bowen, I. D. *Drug Saf.* **1997**, *17*, 149−65.
(9) Matter, B.; Wang, G.; Jones, R.; Tretyakova, N. *Chem. Res. Toxicol.* **2004**, *17*, 731−41.

10.1021/ja058424m CCC: $33.50

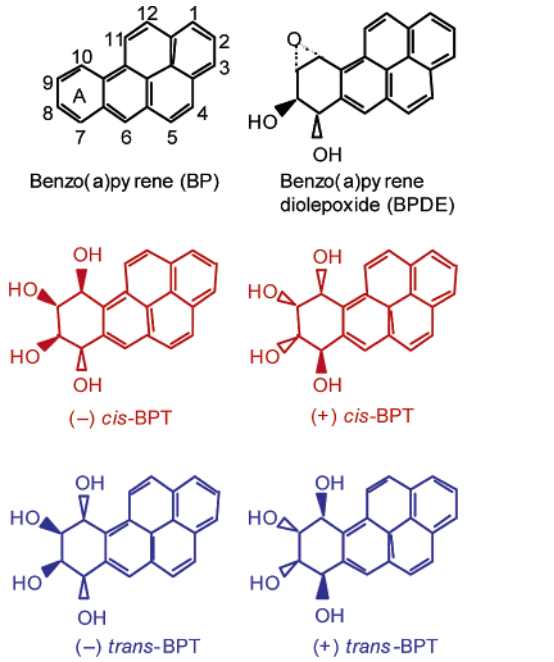

Figure 1. Molecular structures of BP, BPDE, (±) *cis*-BPT, and (±) *trans*-BPT.

Even more, our results reveal that enantiomers can be differentiated due to the changes in their fluorescence spectra resulting from their binding to a promiscuous antibody.

The *anti*-PAH monoclonal antibody (mAb) interacts with a number of polycyclic aromatic hydrocarbons (PAHs), i.e., fluoranthene, pyrene (Py), and benzo[*a*]pyrene (BP).[10] We examine the possibility of exploiting the broad cross-reactivity of the *anti*-PAH mAb for highly specific analysis of biologically important molecules (i.e., dissociation products of B[a]P-derived carcinogen DNA adducts). The two pairs of enantiomers of interest are metabolic derivatives of the mutagenic BP-derived DNA adducts: (±)r-7,t-8,t-9,t-10-tetrahydroxy-7,8,9,10-tetrahydro-benzo[*a*]pyrene (*cis*-BPT) and (±)r-7,t-8,t-9,c-10-tetrahydroxy-7,8,9,10-tetrahydrobenzo[*a*]pyrene or (*trans*-BPT) (Figure 1). It is well-established that BP forms a variety of stable DNA adducts via a monooxygenation metabolic pathway.[9] The stable BP-derived DNA adducts are formed via the bay-region diolepoxide (BPDE) intermediate. The DNA damage-induced mutations to the p53 tumor suppressor gene are believed to be critical for the induction of certain types of chemically induced lung cancers.[11,12] BPTs are of interest as they are the final hydrolytic products of BPDE-derived DNA adducts.[13] Due to the stereoselective biological interaction of BPDE with DNA, the resulting mixture of adducts (and metabolites) derived in in vivo and in vitro experiments consists of a combination of stereoisomers in various ratios,[9] implying different enantiomer activities. While preserving the carbon backbone of the BP molecule, BPTs contain polyhydroxyl moiety residing on the flexible cyclohexenyl ring formed through the metabolic hydroxylation of aromatic ring A of BP (Figure 1).

(10) Grubor, N. M.; Hayes, J.; Small, G. J.; Jankowiak, R. *Proc. Natl. Acad. Sci. U.S.A.* **2005**, *102*, 7453−8.
(11) Denissenko, M. F.; Pao, A.; Tang, M.; Pfeifer, G. P. *Science* **1996**, *274*, 430−2.
(12) Pfeifer, G. P.; Denissenko, M. F.; Olivier, M.; Tretyakova, N.; Hecht, S. S.; Hainaut, P. *Oncogene* **2002**, *21*, 7435−7451.
(13) Kim, S. K.; Brenner, H. C.; Soh, B. J.; Geacintov, N. E. *Photochem. Photobiol.* **1989**, *50*, 327−37.

Here we demonstrate that the binding of enantiomeric *cis*-BPT and *trans*-BPT to the antibody involves different complex geometries. These spatially different ligand−protein interactions alter the excited-state vibrational frequencies of immunocomplexed molecules allowing for unambiguous spectroscopic resolution of all four isomers captured by the antibody. In addition, this study represents the first example of a high-resolution, fluorescence-based spectroscopic method capable of enantiospecific differentiation.

Materials and Methods

Purified *anti*-PAH mAb was purchased from Strategic Biosolutions, Newark, DE. Methanol and glycerol (Aldrich, Milwaukee, WI) were used as received. Phospate-buffered saline (PBS) (0.1 M sodium phosphate and 0.15 M sodium chloride, pH 8.8) was purchased from Pierce and prepared according to the procedure supplied by the manufacturer. Racemic r-7,t-8,t-9,t-10-tetrahydroxy-7,8,9,10-tetrahydro-benzo[*a*]pyrene ((±)*cis*-BPT) and (±)r-7,t-8,9,c-10-tetrahydroxy-7,8,9,-10-tetrahydro-benzo[*a*]pyrene ((±)*trans*-BPT) were purchased from Midwest Research Institute, NCI Chemical Carcinogen Reference Standard Repository, Kansas City, MO.

Pure enantiomers of *cis*- and *trans*-BPT were obtained by semi-preparative HPLC separation of racemic standards on the γ-cyclodextrin chiral stationary phase (Cyclobond II, 250 × 4.6 mm, Astec, Whippany, NJ). The HPLC system consisted of two pumps (LC-10AD, Shimadzu), a UV detector (SPD-6A, Shimadzu), a Chromatopac integrator (CR601, Shimadzu), and a six-port injection valve equipped with a sample loop (10 μL). The detection wavelength was 246 nm, which corresponds to the absorption maxima of the two compounds. The preparative separation conditions used to obtain pure enantiomers of *cis*-BPT and *trans*-BPT are as follows. Racemates of *cis*-BPT and *trans*-BPT were dissolved in methanol to a concentration of 3.2 mg/mL. A 10 μL portion of each sample was injected onto a γ-cyclodextrin column (Cyclobond II, Astec, Whippany, NJ) and eluted with methanol/water, 20/80 (v/v). The enantiomers were collected manually and concentrated under vacuum at 60 °C. The mobile phase was degassed before use, and the flow rate was 1.0 mL/min. A polarimetric detector (Chiralyser, Astec, Whippany, NJ) was used to determine the elution order with a 430 nm wavelength. For both compounds, the (−) enantiomer eluted first, followed by the (+) isomer.

For low-resolution LIF spectroscopic measurements, high-energy laser excitation of 308 nm was provided by a Lambda Physik Lextra 100 XeCl excimer laser. For FLNS measurements, the same laser was used as a pump source for a Lambda Physik FL 2002 Scanmate tunable dye laser system (10 Hz). A 1-m McPherson monochromator (model 2601) and a Princeton Instruments photodiode array were used for dispersion and detection of fluorescence. A Princeton Instruments FG-100 pulse generator was used for time-resolved spectroscopy with detector delay times from 0 to 160 ns and a gate width of 200 ns. For all spectroscopic measurements, 30 μL volumes of sample were placed in quartz tubes and immersed in a helium cryostat with quartz optical windows. To ensure quantitative binding of haptens, immunocomplexes were formed by incubation of a 10-fold excess of antibodies relative to the concentration of haptens ($\sim 10^{-7}$ M) in PBS buffer. All fluorescence spectra are the average of 10 1-s acquisitions unless stated differently. The resolution for FLN and NLN spectra was 0.1 and 0.8 nm, respectively. Corresponding accuracy in vibrational frequencies for FLNS measurements is ± 3 cm^{-1}.

The capillary electrophoresis (CE) experimental setup for binding constant determination by frontal analysis consisted of 257 nm LIF fluorescence detection. UV-transparent capillaries (85 cm × 75 μm i.d. and 365 μm. o.d.) were obtained from Polymicro Technologies and used with a length of 70 cm (55 cm to the detection window). The laser-induced fluorescence detection system consisted of CW excitation at 257 nm provided by a Lexel 95-SHG laser operated at an intensity

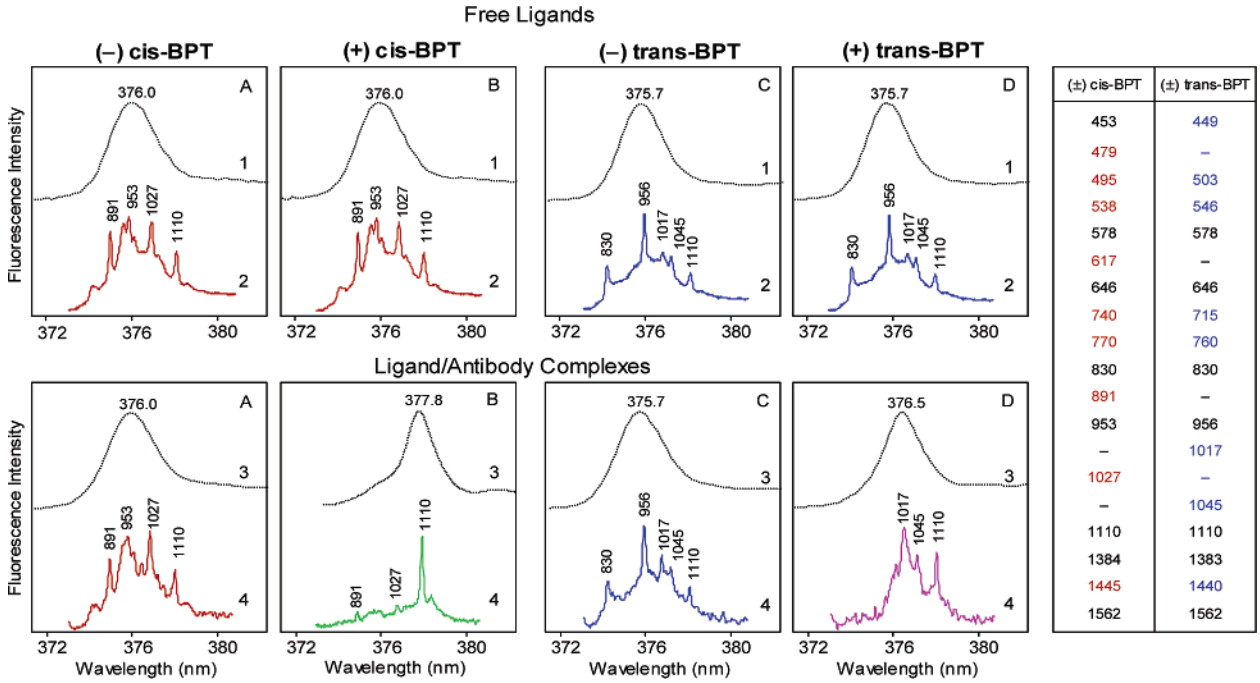

Figure 2. Frames A−D refer to (−) *cis*-BPT, (+) *cis*-BPT, (−) *trans*-BPT, and (+) *trans*-BPT, respectively. $T = 4.2$ K, gate width = 200 ns, gate delay = 40 ns. NLN/FLN spectra of free and immunocomplexed BPT are labeled 1/2 and 3/4, respectively. Vertically oriented numbers label excited-state vibrational frequencies (in wavenumbers; $\Delta\nu = \pm 3$ cm^{-1}) calculated as the differences between the laser excitation frequency and the frequency of the narrow emission line in the corresponding FLN spectrum. In addition to vibrational frequencies labeled in the given spectra, the table lists the most prominent excited-state vibrational frequencies of *cis*-BPT and *trans*-BPT obtained with different laser excitations in the region from 355 to 371 nm (spectra not shown). Values given in red and blue are the frequencies exclusively characteristic for *cis*-BPT and *trans*-BPT isomers, respectively.

of 100 mW. Fluorescence was collected with an objective (N.A. 0.28), dispersed by a monochromator and detected by an intensified CCD camera (Princeton, NJ). Electropherograms were generated by on-line integration of the 320−450 nm spectral region in the fluorescence emission window using WinSpec/32 software, Roper Scientific. The CE running buffer used was 50 mM sodium phosphate buffer at pH 8.8. Sodium phosphate and phosphoric acid were purchased from Fisher Scientifics (Fair Lawn, NJ) and were used for the preparation of a running buffer. The buffer was filtered through 0.22 mm nonpyrogenic filter (Costar Corp., Corming, NY). All buffers and samples were prepared using water purified by a Milli-Q Water Purification System (Millipore). For the frontal analysis, samples were hydrodynamically injected with 20-mbar pressure for 3 s, and electrokinetic separations were carried out at 21 kV (resulting current 20.0 μA).

Results and Discussion

Electronic spectra of molecules contain information on intrinsic molecular structure and can be used for their identification.[14,15] However, due to thermal spectral broadening, classical room-temperature absorbance and luminescence spectroscopies are not capable of resolving the fine structure of molecular vibronic transitions.[16] As a result, spectroscopic differentiation between structurally related molecules (positional isomers, conformational isomers, and stereoisomers) is generally not possible. Although low-temperature spectroscopy (<10 K) significantly reduces thermal spectral broadening (by narrowing the spectral bands, and thus improving resolution), the contribution from the inhomogeneous broadening precludes observation of the fine vibrational transitions.[16,17]

Spectra A1−D1 of Figure 2 represent the (0−0)-bands of low-temperature (4.2 K), non-line-narrowed (NLN) (low-resolution) spectra of four diastereomeric BPT obtained with a 308 nm excitation source. It is evident that the low-resolution spectra of enantiomeric couples are identical, while small differences in the position of the (0−0)-band (0.3 nm) are only observed in *cis*-BPT relative to *trans*-BPT. Additional minor differences between the spectra of *cis*-BPT and *trans*-BPT can be observed in the vibronic region of their florescence spectra (parts of spectra not shown). However, differentiation based on low-resolution fluorescence spectra can be inconclusive and misleading primarily due to the high influence of the surrounding environment on the molecular spectra (see below). On the contrary, selective vibronic excitation in a FLNS experiment reveals a highly structured pattern of the excited-state vibrational frequencies (characteristic for a given molecule) that can probe changes in the microenvironment of various molecules.

As shown in Figure 2, FLN spectra of enantiomeric (±) *cis*-BPT (spectra A2 and B2) on one side, and (±) *trans*-BPT (spectra C2 and D2) on the other, obtained with $\lambda_{ex} = 363.0$ nm, reveal apparent differences. Several distinctive vibrational frequencies are identified for each isomer: 891 and 1027 cm^{-1} for *cis*-BPT, and 1017 and 1045 cm^{-1} for *trans*-BPT. In addition, several other excitation wavelengths (ranging from 355 to 371 nm) were used, each revealing a different portion of the characteristic S_1 excited-state vibrational frequencies (see table in Figure 2). These numbers are consistent with those obtained

(14) Lakowicz, J. R. *Principles of Fluorescence Spectroscopy*, 2nd ed.; Kluwer Academic/Plenum Publishers: New York, 1999.
(15) Jankowiak, R.; Small, G. J. *Chem. Res. Toxicol.* **1991**, *4*, 256−69.
(16) Jankowiak, R. In *Shpol'skii Spectroscopy and Other Site-Selection Methods: Applications in Environmental Analysis*; Gooijer, C., Ariese, F., Hofstraat, J. W., Eds.; John Wiley and Sons: New York, 2000; pp 235−271.
(17) Heisig, V.; Jeffrey, A. M.; McGlade, M. J.; Small, G. J. *Science (Washington, DC)* **1984**, *223*, 289−91.

previously for BPDE-derived DNA adducts and metabolites[18,19] and can be used to positively identify stereoisomeric BPT.

Nevertheless, enantiomers do not reveal spectral differences even under high-resolution conditions, as evident from virtually identical FLN spectra obtained for enantiomeric couples (spectra A2 and B2 for (−) *cis*-BPT and (+) *cis*-BPT, and spectra C2 and D2 for (−) *trans*-BPT and (+) *trans*-BPT, respectively). Importantly, upon complexation of enantiomeric BPT with *anti*-PAH mAb, significant differences are observed in the position of the (0−0)-bands in low-resolution spectra of all four immunocomplexed ligands. While (−) enantiomers of BPT did not reveal notable spectral changes upon complexation (spectra A3 and C3) relative to the spectra of uncomplexed ligands (spectra A1 and A3), spectra of immunocomplexed (+) enantiomers, compared to uncomplexed forms, exhibited significant red wavelength shifts (1.8 nm for (+) *cis*-BPT and 0.8 nm for (+) *trans*-BPT, spectra B3 and D3, respectively). Alterations of molecular electronic spectra arising from interaction of chromophores with the adjacent surrounding medium are commonly observed. Relative intensities of spectral vibronic bands, as well as the spectral band shifts (solvatochromic effect) in electronic spectra of many molecules, are heavily influenced by the properties of their immediate environment, i.e., polarity, dielectric constant, dipole moment, electrostatic interactions.[14] Analogously, complexation of small chromophoric molecules with protein binding sites can induce similar spectral changes. Protein complexation relies on a variety of noncovalent binding interactions, the most important being hydrogen-bond, hydrophobic, van der Waals', and electrostatic interactions.[20] Depending on the molecular structure of its counterpart, an Ab-binding site accommodates an amino acid sequence and geometry to favor specific intermolecular interactions and strong, reversible binding. Alternatively, there are cases where electrostatic and hydrogen bonding is limited or not possible, and the complexation is restricted to other, less spatially directed interactions. As demonstrated recently, $\pi-\pi$ interactions within the antibody pocket are responsible for the binding and broad cross-reactivity of *anti*-PAH mAb and enable its strong binding to a number of different PAHs.[10] Hence, the expected interaction of BP tetrols with *anti*-PAH mAb is through the pyrene moiety that remains free from chemical modification and, thus, is available for interaction with the antibody-binding site. However, four hydroxyl groups residing on the cyclohexenyl ring of BP tetrols may involve additional steric interactions that can enable or hinder a molecule's favorable orientation and interaction with the antibody-binding site.

Indeed, on the basis of the red spectral shift observed in the low-resolution spectra of (+) enantiomers of *cis*-BPT/mAb and *trans*-BPT/mAb complexes, the immunocomplexed pyrene moiety experiences significant $\pi-\pi$ interactions, suggesting ligand inclusion into the binding pocket. As previously described,[10] the environment directing high π-electron density upon the π-electron cloud of the pyrene chromophore shifts its origin band spectral envelope to higher wavelengths (red shift of the (0−0)-band). In FLN spectra, this is reflected in the change of relative intensities of the characteristic vibronic bands, as observed in spectra B4 and D4 of Figure 2 when compared to spectra of uncomplexed forms B2 and D2, respectively. Importantly, the changes in the energy difference between the S_1 and the ground electronic states induced by complexation did not alter the absolute values of the excited-state vibrational frequencies (i.e., no shifts of excited-state vibrational frequencies are observed). The preservation of vibrational frequencies is important since it enables positive identification of a ligand regardless of its residence environment, while the alterations in the relative intensity of those frequencies enable differentiation between isomers that interact with the protein molecule through a different geometrical arrangement.

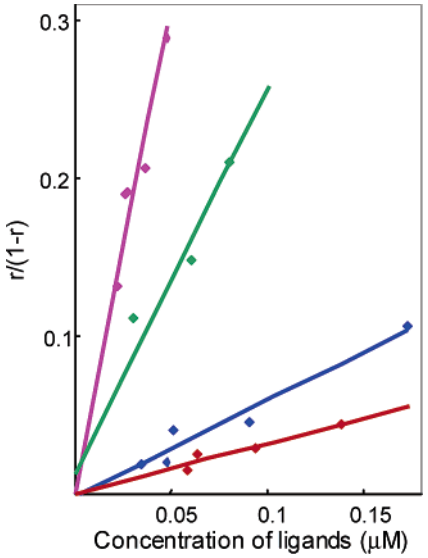

Figure 3. Plot of $r/(1-r)$ against the concentration of free ligands, where r is the fraction of ligand bound per MAb. The association constants (K_a's) for various BPT/*anti*-PAH MAb complexes are derived from the slopes of the linear regression lines: (+) *trans*-BPT, pink line, $K_a = 6.0 \times 10^6\ M^{-1}$; (+) *cis*-BPT, green line, $K_a = 2.4 \times 10^6\ M^{-1}$; (−) *trans*-BPT, blue line, $K_a = 6.1 \times 10^5\ M^{-1}$; (−) *cis*-BPT, red line, $K_a = 2.1 \times 10^5\ M^{-1}$.

For (−) enantiomers, no significant spectral changes are observed upon association with the antibody molecules (spectra A4 and C4), suggesting negligible $\pi-\pi$ interactions directed toward the pyrenyl moiety of (−) *cis*-BPT and (−) *trans*-BPT, respectively. In this case, the lack of spectral alterations does not necessarily imply the complete absence of intermolecular interactions; the possibility of alternative mAb/BPT complex geometries (i.e., more solvent exposed ligand) must be considered.

To correlate the spectral behavior of complexed ligands with their binding strengths (and geometry), and to determine whether binding occurs for all mAb/ ligand pairs, affinity constants for each mAb/ligand complex were determined using the frontal analysis (FA) method of capillary electrophoresis (CE).[21] Figure 3 shows the plot of the $r/(1-r)$ against the concentration of free ligands (where r is the fraction of ligand bound per mAb) for the series of CE injections of four Ab−ligand mixtures. Numerical values for association constants (K_a's) for (+) *trans*-BPT, (−) *trans*-BPT, (+) *cis*-BPT, and (−) *cis*-BPT (calculated from the slopes) are 6.0×10^6, 6.1×10^5, 2.4×10^6, and $2.1 \times 10^5\ M^{-1}$, respectively.

(18) Devanesan, P. D.; RamaKrishna, N. V.; Todorovic, R.; Rogan, E. G.; Cavalieri, E. L.; Jeong, H.; Jankowiak, R.; Small, G. J. *Chem. Res. Toxicol.* **1992**, *5*, 302−9.
(19) Suh, M.; Ariese, F.; Small, G. J.; Jankowiak, R.; Liu, T. M.; Geacintov, N. E. *Biophys. Chem.* **1995**, *56*, 281−96.
(20) Mian, I. S.; Bradwell, A. R.; Olson, A. J. *J. Mol. Biol.* **1991**, *217*, 133−51.
(21) Rundlett, K. L.; Armstrong, D. W. *Electrophoresis* **2001**, *22*, 1419−1427.

The (+) enantiomers of diastereomeric tetrols exhibit significantly higher values for the binding constants relative to their enantiomeric counterparts, which is in agreement with results obtained from the spectroscopic studies described above. However, a larger red spectral shift of the (0−0)-band in the case of (+) *cis*-BPT/mAb complex (1.8 nm) relative to the (+) *trans*-BPT/mAb complex (0.8 nm) did not reveal a higher binding constant. The stronger binding of the (+) *trans*-BPT isomer can be rationalized through the additional stabilization of the immunocomplex due to favorable steric and electrostatic interactions of a flexible tetrahydroxy-cyclohexenyl moiety with the amino acid assembly guarding the gate of the hydrophobic pocket.

Lower binding constants and the lack of spectral changes in the case of complexes of the (−) enantiomers suggest weaker interactions with the antibody; in this case, it is likely that the pyrenyl moiety of BPTs resides, at least partially, out of the antibody binding pocket and is more exposed to the solvent. Such geometry could explain both lower association constants for these enantiomers with the antibody as well as the lack of immediate influence of antibody/BPT complexation on fluorescence spectra of BPTs.

Moreover, electrophoretic mobility shifts and band broadening in an immunoaffinity CE experiment (not shown) indicate lower mass transfer rates for complexes of (+) enantiomers relative to their (−) analogues.[22] Lower mass transfer suggests different kinetics and geometry and presents additional supporting evidence for the inclusive nature of complexes of the (+) enantiomers with *anti*-PAH mAb.

Conclusions

It is demonstrated that the high-resolution fluorescence spectroscopy allows for diastereomeric and enantiomeric discrimination of closely related BP-tetrols complexed with promiscuous antibodies. The differentiation is possible since distinct geometrical arrangements of immunocomplexed stereoisomers lead to shifts of their electronic transitions and subsequent changes in the intensity distribution of their vibrational frequencies. This demonstrated approach not only exhibits potential for chiral differentiation, but also has implications in reaching the ultimate specificity of otherwise cross-reactive immunoassays by discriminatively identifying various species immunocomplexed with a promiscuous antibody.

Acknowledgment. This work was supported by NCI Grant 2PO1 CA 49210-12. Partial support was also provided by the NIH RO1 GM53825-10 and the NIH COBRE award 1 P20 RR15563, and matching support from the State of Kansas.

JA058424M

(22) Grubor, N. M.; Armstrong, D. W.; Jankowiak, R. *Electrophoresis* **2006**, 27, 1078−1083.